Quah, Conal and Yeoman, Mark S. and Cizinauskas, Andrius and Cooper, Kevin and McNally, Donal and Boszczyk, Bronek (2014) Finite element investigation of the effect of spina bifida on loading of the vertebral isthmus. Spine Journal, 14 (4). pp. 675-682. ISSN 1529-9430

Finite Element investigation of the effect of spina bifida on loading of the vertebral isthmus

Conal Quah, Mark S Yeoman, Andrius Cizinauskas, Kevin Cooper, Donal McNally, Bronek Boszczyk

Background:

Spondylolysis (SL) of the lower lumbar spine is frequently associated with spina bifida occulta (SBO). There has not been any study that has demonstrated biomechanical or genetic predispositions to explain the coexistence of these two pathologies. In axial rotation, the intact vertebral arch allows torsional load to be shared between the facet joints. In SBO, the load cannot be shared across the arch, theoretically increasing the mechanical demand of the vertebral isthmus during combined axial loading and rotation when compared to the normal state.

Purpose:

To test the hypothesis that fatigue failure limits will be exceeded in the case of a bifid arch, but not in the intact case, when the segment is subjected to complex loading corresponding to normal sporting activities.

Study Design:

Descriptive Laboratory Study

Methods:

Finite element models of natural and SBO (L4-S1) including ligaments were loaded axially to 1kN and were combined with axial rotation of 3°. Bilateral stresses, alternating stresses and shear fatigue failure on intact and SBO L5 isthmus were assessed and compared.

Results:

Under 1kN axial load, the von Mises stresses observed in SBO and in the intact cases were very similar (differences <5MPa) having a maximum at the ventral end of the isthmus that decreases monotonically to the dorsal end. However, under 1kN axial load and rotation, the maximum von Mises stresses observed in the ipsilateral L5 isthmus in the SBO case (31MPa)

was much higher than the intact case (24.2MPa) indicating a lack of load sharing across the vertebral arch in SBO.

When assessing the equivalent alternating shear stress amplitude, this was found to be 22.6 MPa for the SBO case and 13.6 MPa for the intact case. From this it is estimated that shear fatigue failure will occur in less than 70,000 cycles, under repetitive axial load & rotation conditions in the SBO case, while for the intact case, fatigue failure will occur only over 10 million cycles.

Conclusion:

SBO predisposes spondylolysis by generating increased stresses across the inferior isthmus of the inferior articular process, specifically in combined axial rotation and anteroposterior shear.

Clinical Relevance:

Athletes with SBO who participate in sports that require repetitive lumbar rotation, hyperextension and/or axial loading are at a higher risk of developing spondylolysis compared to athletes with an intact spine.

Key Terms:

Spina Bifida Occulta, spondylolysis, finite element analysis, stress fracture, fatigue fracture, lumbar spine

What is known about the subject:

SL of the lower lumbar spine is frequently associated with SBO. A recent investigation has revealed a 3.7 fold Odd ratio for the presence of SL in individuals with SBO. As yet, it is unclear if SBO is a predisposition for the development of SL.

What this study adds to existing knowledge:

Our study suggest that SBO increases load across the pars and does predispose to early fatigue fracture, especially in athletes involved in activities requiring repetitive hyperextension loading. We feel that the mechanical factors play a more important role in the increased incidence of SL in patients with SBO than genetic factors.

Introduction

Spondylolysis (SL) of the lower lumbar spine is frequently associated with spina bifida occulta (SBO). A recent investigation has revealed a 3.7 fold Odd ratio for the presence of SL in individuals with SBO.[21] As yet, it is however unclear if SBO is a predisposition for the development of SL. While SBO is a congenital defect, SL is recognised as being a fatigue fracture with an increased incidence among athletes participating in disciplines requiring repetitive forceful hyperextension, axial loading and rotation.[10, 13, 18, 20, 24] In theory, the presence of SBO impairs load sharing across the vertebral arch and increases the load on the isthmus especially in axial rotation.

We hypothesise that shear fatigue failure limits will be exceeded in the case of a bifid arch, but not in the intact case, when the segment is subjected to complex loading corresponding to normal sporting activities.

The aim of this finite element (FE) investigation therefore is to analyse the effect of SBO on the load of the vertebral isthmus in a combination of loading patterns typical for sports associated with SL – specifically detailing load distribution patterns of the ipsi- and contralateral vertebral isthmus in combined axial loading and rotation.

Methods and Materials

A three-dimensional, non-linear FE-model of an intact L4-S1 human lumbar motion segment including ligaments was used in this study (Figure 1). Validation of the intact three-dimensional lumbar model has been done against the work of Zhu et al.[29] The intact three-dimensional model was adapted to mimic the spina bifida occulta condition by removing a section of the L5 vertebral arch and spinous process, as illustrated in Figure 2. The sacral slope which represents the angle between the sacral plate and the horizontal line of both models were orientated to 66% mimicking the degree of sacral slope in athletes with a high pelvic incidence.[12, 25] A commercial software package COMSOL 3.5a, was used to perform the finite element analysis. The models consisted of two vertebrae, the inter-vertebral disc, and the following ligaments; intertransverse, facet capsule, flaval, supraspinous, interspinous, anterior and posterior longitudinal ligaments. For the SBO condition, the supraspinous and interspinous ligmaments where obviously not considered.

The inner and outer Annulus fibrosis regions of the intervertebral disc were modelled with orthotropic material models using a cylindrical co-ordinate system in line with the central axis of the inter-vertebral disc. The nucleus was modelled as a low modulus nearly incompressible body with a stiffness of 1MPa and Poisson's ratio of 0.499. The ligaments were represented by shell elements with linear elastic material relationships. The shell elements allowed for loading in tension but buckled under compression. The articulating facet surfaces were modelled with cartilage regions and utilised a surface contact penalty algorithm with a normal penalty contact factor of $5x10^{11}$ Pa/m and the surfaces were considered frictionless (zero coefficient of friction). The facet cartilage region was assumed to have a thickness of 0.6 mm and was initially in point contact. The capsular ligaments were modelled with shell elements.

The cancellous regions of the vertebral bodies for both models were meshed using 4-noded tetrahedral elements, while the cortical region of the vertebral bodies and the ligaments were modelled using Mindlin-Reissner shell elements. The cortical region was modelled with 2.5mm thick shells while the ligaments were modelled with 2mm thick shells. Both the 4-noded tetrahedral and Mindlin-Reissner shell elements were meshed with a maximum element size of 3mm.

Two loading conditions were studied: an axial load of 1kN applied to superior vertebral endplate of L4, and the same axial load combined with a 3° axial rotation (rotation of spinal processes of L4 toward left lateral side when viewed from posterior) (Figure 3). Note that axial loading of L4 results in a component of AP shear at both the L4-5 and L5-S1 disc spaces. Stresses (von Mises) and strains on both ispsilateral and contralateral inferior lines of the L5 isthmus as illustrated in Figure 4 were assessed and compared. Graphs were then plotted with the length of the isthmus represented in percentage, where zero represents the ventral end of the isthmus line, close to the veterbral body. In addition, we calculated the mean stress and alternating stresses from the observed 1st and 3rd principle stresses. Goodman diagrams and the Soderberg relationship were then used to relate stress amplitude and mean stress to an equivalent alternating shear stress.[14, 23, 30]

The failure characteristics of human cortical bone have been studied extensively. Cortical bone has a shear strength that is considerably smaller than compressive or tensile strength.[8, 30] It is therefore usual for bone to fail in shear. Furthermore, the shear strength of bone reduces with the number of loading cycles to which it is subjected – it fatigues. This fatigue

behaviour has been characterised by Zioupos et al. in the form of Wöhler curves (or S-N Curves).[30] It is possible to predict either the fatigue strength (S) or the number of cycles to failure (Nf) using the relationship:

$$S = So + Sr \log(Nf) \quad (1)$$

and

So = 36.6 MPa (Shear Strength in a single cycle failure)

Sr = -2.9 MPa

From this relationship, a shear stress of more than 36.6 MPa will result in failure in a single cycle, 19.2MPa at 1 million cycles and 16.3 MPa at 10 million cycles.

Results

Axial Loading

Because the L4-5 and L5-S1 disc spaces are not parallel to the L4 superior endplate (where the load is applied), there is a component of shear loading between L4 and L5 and L5 and S1. This loading is resisted by the intervertebral discs but also by the facet joints. For L5, the superior facets are loaded (by L4) in an anterolateral direction whilst the inferior facets are loaded (by S1) in a posteromedial direction. This turning moment results in twisting of the pedicles (left pedicle anticlockwise when viewed from posteriorly, right pedicle clockwise). The bridge formed by the posterior arch will be compressed by such loading, but will share loading with the pedicles. Hence, in the case of SBO, the pedicles experience greater torsional forces and therefore the shear stress along the isthmus is expected to be greater.

This effect is masked when von Mises stresses are considered (Figure 5a). Von Mises stresses in the intact and SBO cases are very similar (differences <5MPa) having a maximum at the ventral end of the isthmus that decreases monotonically to the dorsal end (Figure 5a, Table 1).

Combined axial loading and rotation

Axial rotation is resisted within the lumbar spine by the posterior portion of the articular facets; the ipsilateral facets are loaded in compression (via the articular surfaces) whilst the contra-lateral joints are loaded in tension (via the capsular ligaments). [3] Such loading of the superior and inferior facets generates twisting moments about the pedicles. However, unlike

the shear case above, these moments are in the same direction for both pedicles (anticlockwise when viewed from posterior with rotation of the superior vertebrae to the left as in Figure 3).

In the intact case, the posterior bridge (vertebral arch) prevents the pedicles from twisting independently; a coupled motion of the entire segment is produced instead. In terms of lateral rotation the ipsilateral joints are free to translate superiorly, whereas the contralateral joint capsules are already under tension and hence act as a pivot point. The segment therefore experiences a lateral rotation towards the contralateral side.

In the SBO case, the pedicles are free to rotate independently. There is therefore greater local deformation of the pedicles compared to whole segment motion. It should be remembered that the axial rotation is superimposed upon a forward shear load. In the case of the ipsilateral pedicle (left pedicle) the rotations generated by both act in the same direction and therefore reinforce one another. In the case of the contralateral pedicle (right pedicle) the rotation induced by the shear load is clockwise whilst that from the axial rotation is anticlockwise. The two effects therefore have a tendency to cancel each other out.

We can see that the mechanical behaviour described above is reflected in the von Mises stresses calculated at 3° axial rotation and 1000N axial compression (Figure 5b). The ipsilateral pedicle in SBO experiences higher von Mises stresses from the locations 30-75% from ventral to dorsal along the isthmus line compared to intact. The ability of pedicles to twist independently in SBO has a slightly protective effect on the contralateral pedicle 5-45% from ventral to dorsal along the isthmus line compared to the intact (Figure 5b).

This observation is much clearer from the fatigue stress graph (Figure 6), where the maximum stress amplitude for the ipsilateral SBO and Intact model were 22.5 MPa and 13.6 MPa respectively.

Fatigue Failure

We can test out our hypothesis that SBO predisposes fatigue failure of the isthmus by considering Figure 6 which is a graph of maximum shear stress amplitude along the inferior L5 istmus whilst rotating axially from 3° left to 3° right under 1000 N axial load. As noted previously, we can expect fracture initiation within 10 million cycles if this parameter exceeds 16.3 MPa. In the intact case, shear stress amplitude remains below 14 MPa and is

therefore unlikely to experience fatigue failure. Whereas the SBO case peaks at 22.5 MPa at a position 57% of the way from ventral to dorsal along the isthmus line. This magnitude of shear stress corresponds to failure after 70,000 cycles. Figure 7 (location of shear stress exceeding 10^6 cycle threshold) is a representation of the locations along the isthmus line where fatigue failure is predicted to occur in less than 1 million cycles.

Discussion

Our results strongly support the hypothesis that SBO predisposes SL by generating increased stresses across the inferior isthmus of the inferior articular process, specifically in combined axial rotation and posterior anterior shear. We demonstrated that reasonable physiological loading leads to focal regions of shear stress that exceed levels required for fatigue failure located at the point on the isthmus where spondylolytic fractures are initiated in segments with SBO but not in intact specimens. We found that axial loading alone, however, was not sufficient to generate loading that would cause injury. For injury to occur, the axial loading needed to be combined with axial rotation.

Several finite element studies of an intact spine have demonstrated much higher stress magnitudes in the pars interarticularis than other regions along the vertebral arch under simulated loads.[4, 5, 26] Chosa et al. carried out a biomechanical study of lumbar SL using three dimensional finite element analysis and concluded that the stress in the pars interarticularis was high particularly under extension and rotation.[4] Other studies have also reported similar findings which suggest combined movements of hyperextension, rotation and axial stress are relatively high risk factors that can lead to SL.[22] Our results are broadly congruent with the only other finite element analysis by Sairyo et al that specifically made a biomechanical comparison of the lumbar spine with and without SBO.[19] This study only reports von Mises stresses at the ventral and dorsal cortex of the pars interarticularis (the former corresponding to the dorsal end of the isthmus in our study). We predict very similar magnitudes of stress at this point 7.4-8.6 MPa vs. 10.6-12.3 MPa (ipsilateral) and 1.7-6.5 MPa vs. 3.8-4.6 MPa (contralateral). The small differences can be attributed to differences between the geometry and loading conditions in the two models. The conclusion we draw, that SBO changes the loading of the vertebra in a way that will lead to spodylolytic fracture, contrasts to the conclusion of Sairyo that SBO does not influence vertebral biomechanics. This difference must be addressed; fortunately the explanation is actually straightforward. Sairyo only reported loading at two points on the pars interarticularlis, whereas we

considered the full length of the inferior cortex of the pedicle. It can be seen clearly in Figure 6 that we also found no difference in loading between the intact and SBO cases in the same location at the ventral end of the pars. The difference that we observed between the two occurred more ventrally towards the pedicle. Whilst single cycle failure stresses were not observed in any of the models, stresses that correspond to shear fatigue failure after 70,000 cycles of repetitive axial load and rotation conditions in the SBO case were observed. For the intact case, fatigue failure will only occur over 10 million cycles. Clearly, for such an observation to be clinically significant, the magnitude and number of cycles to failure need to be placed within an appropriate physiological context.

The axial load applied to the segment was 1 kN; this can be placed in context by using *in vivo* measurements of intradiscal stress under normal activities and ex vivo measurements of intradiscal stress under axial loading applied to isolated spinal segments.[1, 9, 27] These studies suggest that activities such as jogging in normal shoes, standing leaning forward and holding a 20kg weight close to the body correspond to segment axial loads of approximately 1 kN. The magnitude and number of loading cycles (but without the axial rotation critical to fracture initiation) that we predict will initiate spondylolytic fracture therefore corresponds to seven 10k runs. A 45° axial trunk rotation has been shown to result in a 1.7° and 1.6° axial rotation at L4-5 and L5-S1 respectively.[7] In our study we applied a rotation of 3° over these two levels, which would therefore correspond to a 41° trunk rotation. Clearly this level of trunk rotation is common in a wide range of sporting and daily activities. It is therefore entirely reasonable to expect that a sportsman will exceed, in terms of axial load, axial rotation and number of cycles, the conditions that will lead to spondylolytic fracture in cases of SBO.

The prevalence of lumbar SL is higher in athletes (8%) when compared to the general population (3-6%).[6, 24, 28] Athletes who are involved in sports such as cricket, gymnastics, swimming or American football are at a particular risk of developing SL due to the repetitive lumbar rotation, hyperextension and/or axial loading.[10, 13, 24] SBO is a benign clinical condition which is often present in patients with SL.[15] It occurs most commonly in the lumbosacral junction with an estimated incidence of 20% in the general population.[8] Despite a high correlation of SBO in the spondylolytic population, there has not been any study that has demonstrated any biomechanical or genetic predispositions to explain the coexistence of these two pathologies.[11, 15] This is the first study that has provided a biomechanical mechanism by which SL of the lower lumbar spine is predisposed by SBO.

Athletes with SBO who are keen to get involved in these high risk sports at a professional level should be counselled appropriately as our results suggest that they are at an increased risk for developing SL when compared to athletes with an intact spine. SL can be treated conservatively with early diagnosis however will require a prolonged period of rest from training and competition ultimately resulting in loss of playing time. Injury surveillance instigated by the governing bodies of professional cricket in Australia and United Kingdom have shown that the specific diagnosis which result in the loss of playing time for professional fast bowlers are lumbar stress injuries such as SL and spondylolisthesis.[16] This creates a serious problem particularly for professional athletes. As SBO is quite often an incidental finding on X-rays, screening athletes for SBO who are interested in taking up high risk sports professionally may be an option in the future so that the individual can be counselled appropriately. Radiographs of the lumbar spine in certain sports such as college football have already been a standard part of the preparticipation athletic physical in some universities.[10] The coach, trainer and team physician can then prescribe the appropriate technique, workload, exercise regime and playing position to improve the athlete's performance and safety.

Several limitations of this study should be recognised. This study used constant axial load of 1kN to represent both muscle and gravitational forces. This is clearly a considerable simplification, however this assumption does allow direct, like with like, comparison of all cases. The remodelling potential of the vertebral body, resulting from a congenital deformity, was not taken into consideration. Again this is a simplification that allows direct comparisons between cases to be made. We also assumed that the gap in the pars defect, which has been shown to fill with lysis tissue did not transmit loads. This is a reasonable assumption to make since such tissue has been shown not to withstand external shear forces.[2] These assumptions have not prevented this lumbar spine FEA model from gaining a better understanding of altered load transfer in combined axial rotation and anteroposterior shear in SBO**.** There should be further research to analyse the influence of pelvic incidence in developing SL, as the variation in pelvic incidence may further effect the loading characteristics across the isthmus.[17]

In conclusion, our FE results suggest that SBO increases load across the pars and does predispose to early fatigue fracture, especially in athletes involved in activities requiring repetitive hyperextension loading. We feel that the mechanical factors play a more important role in the increased incidence of SL in patients with SBO than genetic factors.

Screening for SBO in athletes who participate in high risk sports may have a role to play in professional sports.

Reference

1) Adams MA, McMillan DW, Green TP, Dolan P. Sustained loading generates stress concentrations in lumbar intervertebral discs. *Spine*. 1996;21(4):434–438.

2) Boszczyk BM, Boszczyk AA, Boos W, Korge A, Mayer HM, Putz R, et al. An immunohistochemical study of the tissue bridging adult spondylolytic defects--the presence and significance of fibrocartilaginous entheses. *Eur Spine J.* 2006 Jun;15(6):965-71.

3) Boszczyk BM, Boszczyk AA, Putz R, Buttner A, Benjamin M, Milz S.An immunohistochemical study of the dorsal capsule of the lumbar and thoracic facet joints.*Spine*. 2001 Aug 1;26(15):E338-43.

4) Chosa E, Totoribe K, Tajima N. A biomechanical study of lumbar spondylolysis based on a three-dimensional finite element method. *J Orthop Res*. 2004 Jan;22(1):158-63.

5) Dietrich M, Kurowski P. The importance of mechanical factors in the etiology of spondylolysis. A model analysis of loads and stresses in human lumbar spine*. Spine.* 1985 Jul-Aug;10(6):532-42.

6) Fredrickson BE, Baker D, McHolick WJ, Yuan HA, Lubicky JP. The natural history of spondylolysis and spondylolisthesis. *J Bone Joint Surg Am*. 1984 Jun;66(5):699-707.

7) Fujii R, Sakaura H, Mukai Y, Hosono N, Ishii T, Iwasaki M, Yoshikawa H, Sugamoto K. Kinematics of the lumbar spine in trunk rotation: in vivo three dimentional analysis using magnetic resonance imaging. *Eur Spine J*. 2007 Nov;16(11):1867-74

8) Ganey TM, Odgen JA. Development and maturation of the axial skeleton. In: Weinstein SL (ed). The Pediatric Spine. 2nd edn. Lippincott Williams and Wilkins: Philidelphia, PA 2001, pp 3-54.

9) Heuer F, Schmidt H, Claes L, Wilke HJ. Stepwise reduction of functional spinal structures increases vertebral translation and intradiscal pressure. *J Biomech*. 2007; 40(4):795-803.

10) Jones DM, Tearse DS, el-Khoury GY, Kathol MH, Brandser EA. Radiographic abnormalities of the lumbar spine in college football players. A comparative analysis. *Am J Sports Med*. 1999 May-Jun;27(3):335-8.

11) Kettelkamp DB, Wright DG. Spondylolysis in the Alaskan Eskimo. *J Bone Joint Surg Am*. 1971 Apr;53(3):563-6.

12) Mac-Thiong JM, Labelle H, Berthonnaud E, Betz RR, Roussouly P. Sagittal spinopelvic balance in normal children and adolescents. *Eur Spine J*. 2007 Feb;16(2):227-34.

13) Maurer M, Soder RB, Baldisserotto M. Spine abnormalities depicted by magnetic resonance imaging in adolescent rowers. *Am J Sports Med*. 2011 Feb;39(2):392-7.

14) Mechanics of Materials, Volume 2 - An Introduction to the Mechanics of Elastic and Plastic Deformation of Solids and Structural Materials (3rd Edition) E.J. Hearn, Elsevier, 1997.

15) Oakley RH, Carty H. Review of spondylolisthesis and spondylolysis in paediatric practice. *Br J Radiol.* 1984 Oct;57(682):877-85.

16) Orchard J, James T, Alcott E, Carter S, Farhart P. Injuries in Australian cricket at first class level 1995/1996 to 2000/2001.*Br J Sports Med*. 2002;36(4):270-4.

17) Pierrs R, Gollogly S, Berthonnaud E, Hubert L, Weidenbaum M. Sagittal Alignment of the Spine and Pelvis in the Presence of L5–S1 Isthmic Lysis and Low-Grade Spondylolisthesis. *Spine* 2006;31(21): 2484-2490.

18) Rossi F, Dragoni S. Lumbar spondylolysis: occurrence in competitive athletes. Updated achievements in a series of 390 cases. *J Sports Med Phys Fitness*. 1990 Dec;30(4):450-2.

19) Sairyo K, Goel VK, Vadapalli S, Vishnubhotla SL, Biyani A, Ebraheim N, et al. Biomechanical comparison of lumbar spine with or without spina bifida occulta. A finite element analysis. *Spinal Cord*. 2006 Jul;44(7):440-4.

20) Sairyo K, Katoh S, Sasa T, Yasui N, Goel VK, Vadapalli S, et al. Athletes with unilateral spondylolysis are at risk of stress fracture at the contralateral pedicle and pars interarticularis: a clinical and biomechanical study. *Am J Sports Med*. 2005 Apr;33(4):583-90.

21) Sakai T, Sairyo K, Takao S, Nishitani H, Yasui. N Incidence of lumbar spondylolysis in the general population in Japan based on multidetector computed tomography scans from two thousand subjects. *Spine.* 2009 Oct 1;34(21):2346-50.

22) Schulitz KP, Niethard FU. Strain on the interarticular stress distribution. Measurements regarding the development of spondylolysis. *Arch Orthop Trauma Surg*. 1980;96(3):197-202.

23) Shigley's Mechanical Engineering Design, Eight Edition in SI Units (Mcgraw-Hill Series in Mechanical Engineering), 2008.

24) Soler T, Calderon C. The prevalence of spondylolysis in the Spanish elite athlete. *Am J Sports Med*. 2000 Jan-Feb;28(1):57-62.

25) Swärd L, Hellström M, Jacobsson B, Peterson L. Spondylolysis and the sacro-horizontal angle in athletes. *Acta Radiol*. 1989 Jul-Aug;30(4):359-64.

26) Tajima N, Totoribe K, Chosa E. Biomechanical study of the lumbar spondylolysis using a three-dimensional finite element model and 3D-CT images. *Res Spinal Defor*. 1997(1):185-8.

27) Wilke HJ, Neef P, Caimi M, et al. New in vivo measurements of pressures in the intervertebral disc in daily life. *Spine*. 1999;24(8):755–62.

28) Wiltse LL, Widell EH, Jr., Jackson DW. Fatigue fracture: the basic lesion is isthmic spondylolisthesis. *J Bone Joint Surg Am*. 1975 Jan;57(1):17-22.

29) Zhu Q, Larson CR, Sjovold SG, Rosler DM, Keynan O et.al.. Biomechanical Evaluation of Total Facet Arthroplasty System -3D Kinematics. *Spine*. 2007 Jan 1;32(1):55-62

30) Zioupos P, Gresle M, Winwood K. Fatigue strength of human cortical bone Age physical & material heterogeneity effects. *J Biomed Mater Res A*. 2008 Sep;86(3):627-36

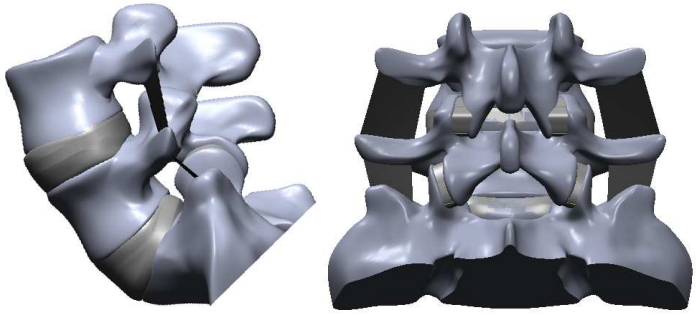

Figure 1: Natural L4-5 model in a lateral and posterior view with intact vertebral arch.

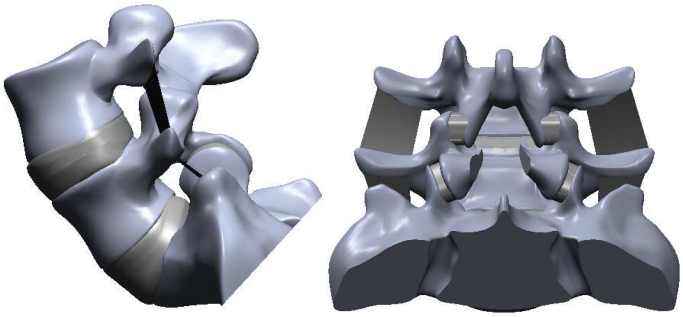

Figure 2: Spina Bifida Occulta Model in a view from lateral and posterior with deficient L5 vertebral arch.

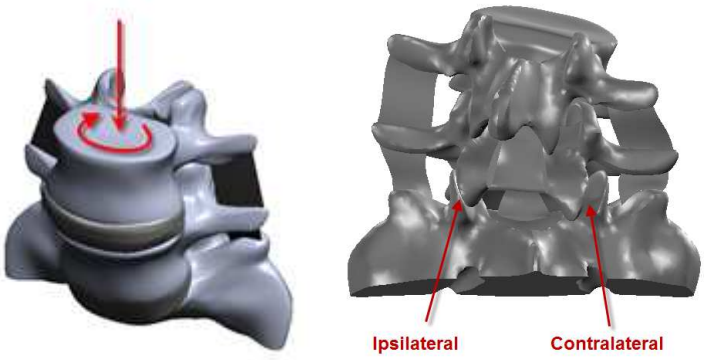

Figure 3: Image of SBO model illustrating load conditions and direction of axial rotation & deformed image of SBO model illustrating ipsilateral & contralateral sides

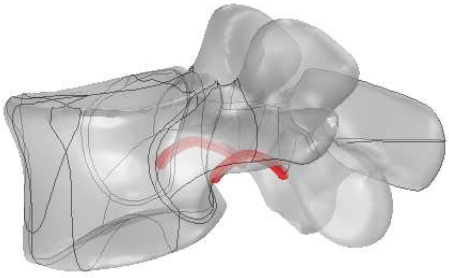

Figure 4: Inferior L5 isthmus lateral lines used to obtain results

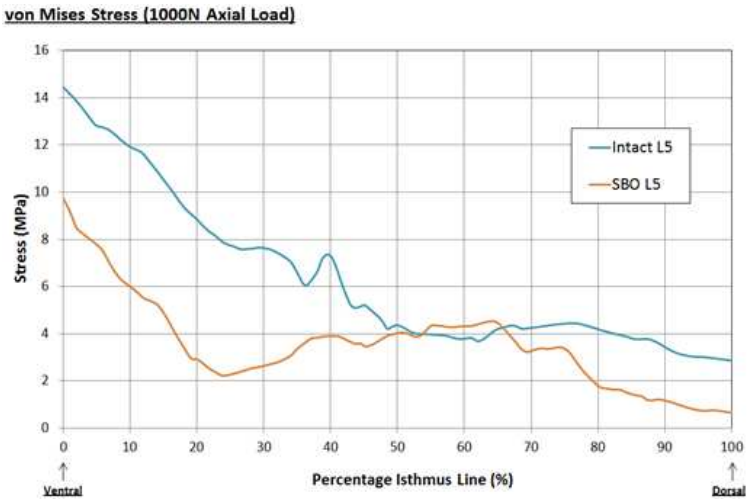

Figure 5 : von Mises stresses, on inferior lateral lines of the L5 isthmus in 1000N axial load only.

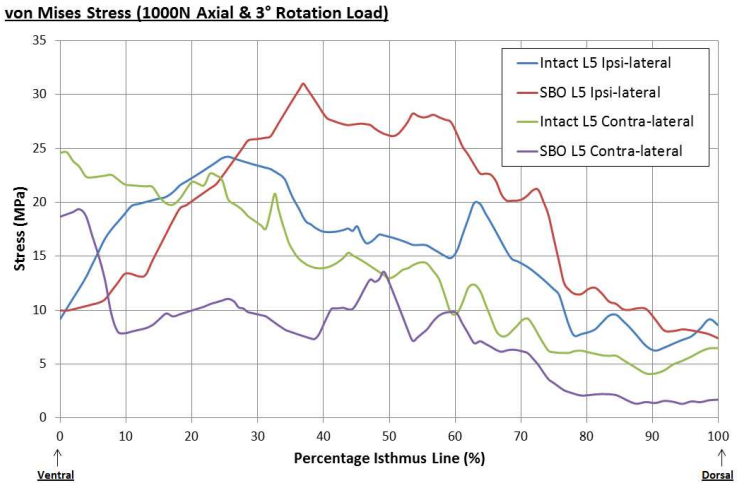

Figure 5b : von Mises stresses, on inferior lateral lines of the L5 isthmus with 1000N axial and 3° rotation load.

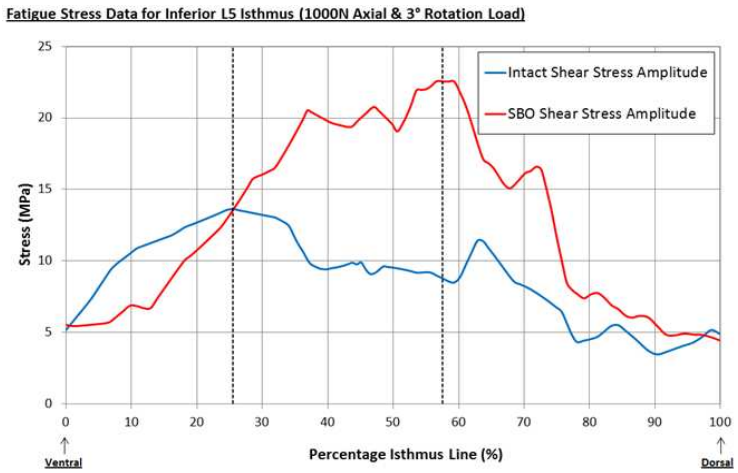

Figure 6: Graphs of Alternating Fatigue Stress (Shear) on the inferior lateral lines of the L5 isthmus

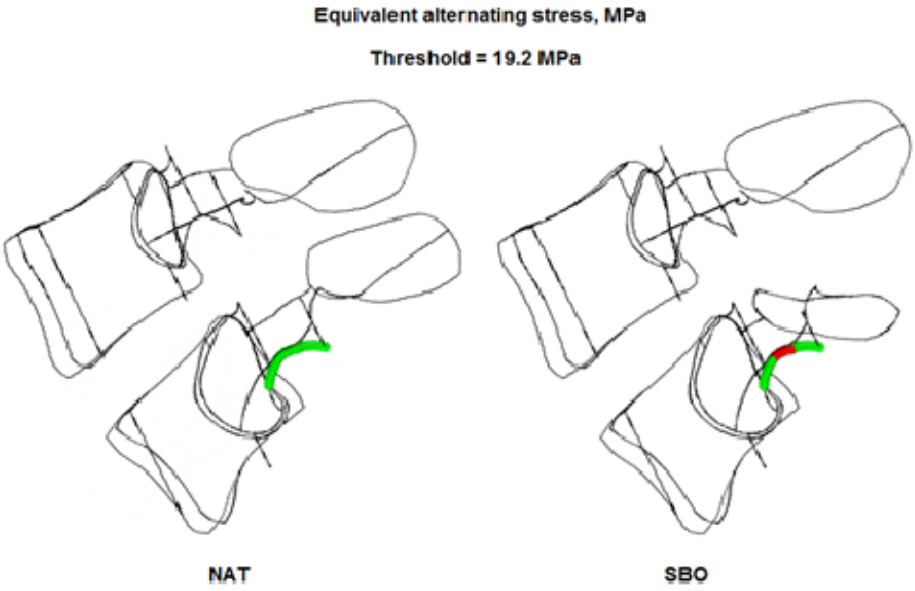

Figure 7: Representation of the location along the L5 isthmus line where fatigue failure is predicted to occur in less than 1 million cycles

Region	1000N Axial Load Only			1000N Axial Load & 3° Rotation					
				Ipsilateral			Contralateral		
	Intact	SBO	% difference between Intact & SBO	Intact	SBO	% difference between Intact & SBO	Intact	SBO	% difference between Intact & SBO
Units	MPa	MPa	%	MPa	MPa	%	MPa	MPa	%
L5 Ventral	14.45	9.72	-32.7	9.2	9.98	8.5	24.66	18.68	-24.2
L5 Dorsal	2.81	0.65	-76.9	8.57	7.37	-14.0	6.47	1.69	-73.9
L5 Max	14.45	9.72	-32.7	24.24	31.03	28.0	24.66	19.37	-21.5

Table 1: von Mises stress on Cortical Bone at Ventral & Dorsal Points on the inferior L5 isthmus. L5 max represents the point of maximum stress observed along the inferior L5 istmus.